MIT Open Access Articles

Systems-pharmacology dissection of a drug synergy in imatinib-resistant CML

Massachusetts Institute of Technology

Systems-pharmacology dissection of a drug synergy in imatinib-resistant CML

Georg E Winter[#,1], **Uwe Rix**[#,1,6], **Scott M Carlson**[2,6], **Karoline V Gleixner**[3], **Florian Grebien**[1], **Manuela Gridling**[1], **André C Müller**[1], **Florian P Breitwieser**[1], **Martin Bilban**[4], **Jacques Colinge**[1], **Peter Valent**[3,5], **Keiryn L Bennett**[1], **Forest M White**[2], and **Giulio Superti-Furga**[1,*]

[1]CeMM Research Center for Molecular Medicine of the Austrian Academy of Sciences, Vienna, Austria.

[2]Department of Biological Engineering and Koch Institute for Integrative Cancer Research, Massachusetts Institute of Technology, Cambridge, Massachusetts, USA.

[3]Department of Internal Medicine I, Division of Hematology and Hemostaseology, Medical University of Vienna, Vienna, Austria.

[4]Clinical Institute for Medical and Chemical Laboratory Diagnostics, Medical University of Vienna, Vienna, Austria.

[5]Ludwig Boltzmann Cluster Oncology, Vienna, Austria.

[#] These authors contributed equally to this work.

Abstract

Occurrence of the BCR-ABL[T315I] gatekeeper mutation is among the most pressing challenges in the therapy of chronic myeloid leukemia (CML). Several BCR-ABL inhibitors have multiple targets and pleiotropic effects that could be exploited for their synergistic potential. Testing

[*]gsuperti@cemm.oeaw.ac.at.
[6]Present addresses: Department of Drug Discovery, H. Lee Moffitt Cancer Center and Research Institute, Tampa, Florida, USA (U.R.) and Department of Biology, Stanford University, Stanford, California, USA (S.M.C.).

combinations of such kinase inhibitors identified a strong synergy between danusertib and bosutinib that exclusively affected CML cells harboring BCR-ABL^{T315I}. To elucidate the underlying mechanisms, we applied a systems-level approach comprising phosphoproteomics, transcriptomics and chemical proteomics. Data integration revealed that both compounds targeted Mapk pathways downstream of BCR-ABL, resulting in impaired activity of c-Myc. Using pharmacological validation, we assessed that the relative contributions of danusertib and bosutinib could be mimicked individually by Mapk inhibitors and collectively by downregulation of c-Myc through Brd4 inhibition. Thus, integration of genome- and proteome-wide technologies enabled the elucidation of the mechanism by which a new drug synergy targets the dependency of BCR-ABL^{T315I} CML cells on c-Myc through nonobvious off targets.

Redundancy and multifunctionality are inherent characteristics of biological systems that limit the therapeutic opportunity of single-agent applications[1]. Combinations of drugs that yield a synergistic effect are thought to be the most effective way of counter ing biological buffering and also allow reduced dosing of each agent while increasing therapeutically relevant selectivity[2]. Recent advances in assaying the impact of small molecules on the transcriptome or the proteome in terms of drug binding or alterations in post-transcriptional modifications led to a complex picture of drug action that goes against the 'one drug, one target' paradigm[3–5]. Although each of the above-mentioned approaches generates a wealth of useful data, together they only allow for partial insight into the composite effects of small-molecule agents on complex cellular systems. These effects are a consequence of all on- and off-target drug effects and impairment of the related cellular processes, including changes in gene expression[6,7]. As a result of crosstalk at various levels, this complexity is markedly increased if two drugs are applied simultaneously. Deconvolution of the relevant cellular mechanism underlying a combined treatment with two drugs that yields a synergistic and therefore unpredictable effect is a particular challenge.

CML is a clonal hematopoietic disease hallmarked by the expression of the BCR-ABL fusion oncoprotein that results from a reciprocal translocation between chromosomes 9 and 22. BCR-ABL features a deregulated tyrosine kinase activity that drives a number of downstream signaling pathways, confers growth advantage and counteracts apoptosis[8]. The most prominent downstream pathways upregulated by BCR-ABL include the PI3K, STAT5 and MAPK pathways. Treatment of CML rapidly improved after the introduction of the first BCR-ABL inhibitor, imatinib (Gleevec, STI-571), which serves as a paradigmatic example for targeted therapies[9].

Imatinib causes complete remission and prolonged lifespan in the majority of patients with CML[9]. Nevertheless, it soon became apparent that a broad spectrum of possible resistance mechanisms toward imatinib treatment, for example, acquisition of point mutations in the ATP binding pocket or overexpression of LYN or BCR-ABL itself, necessitated the development of second- and third-generation BCR-ABL inhibitors such as nilotinib (Tasigna, AMN107) and dasatinib (Sprycel, BMS-354825)[10–14]. These later-generation agents have been successful in over-riding a broad variety of resistance mechanisms against imatinib. However, none of them is effective in patients with CML who harbor the so-called BCR-ABL 'gate-keeper mutations' at Thr315. Thus, these patients are in need of new

therapeutic approaches, although promising experimental targeting strategies have been reported recently[15–18].

Here we describe a new synergistic interaction between the clinically tested multikinase inhibitors danusertib (PHA-739358) and bosutinib (SKI-606) that is specific for BCR-ABL gatekeeper mut ation–transformed cells. We deciphered the molecular logic underlying the synergistic effect using a multilevel experimental approach that included proteome-wide measurements of drug-binding using chemical proteomics, global monitoring of alterations in phosphorylation states in response to drug treatment and genome-wide transcriptomics. Correlating the affected signaling pathways with drug-dependent transcription-factor signatures revealed reduced c-Myc activity as the key point of convergence.

To the best of our knowledge, this is the first description of a comprehensive dissection of a synergistic drug interaction using three different large-scale 'omics' data sets. In this study, we show that the systems-level cooperative effect obtained by applying danusertib and bosutinib in combination results from previously unappreciated features of both agents. We believe that this strategy of gaining a functional understanding of a drug synergy may serve as a model for further mode-of-action studies.

RESULTS

Identification of synergy specific for BCR-ABL[T315I] cells

The overall experimental strategy is outlined schematically in **Figure 1a**. It starts with point-wise synergy screens and their validation using three-dimensional dose-response surfaces, which is then followed by three parallel experimental lines of investigation: (i) determination of the cellular binding partners of the involved drugs, (ii) mapping the impact of the single agents as well as their combination on the transcriptome and (iii) charting the global changes in the phosphoproteome after drug exposure. Integration of the data sets generates hypotheses that are subsequently validated. We chose to investigate synergies that were specific for gatekeeper mutant–associated imatinib-resistant BCR-ABL. To identify such potential synergistic interactions, we used the Ba/F3 mouse pro-B cell line system that was retrovirally transduced with BCR-ABL[T315I], which conferred interleukin-3–independent growth properties. First, we generated dose-response curves for eight clinical BCRABL inhibitors known to be sufficiently safe in the relevant patient class (imatinib, nilotinib, dasatinib, bosutinib, bafetinib, tozasertib, danusertib and sorafenib). Most of the tested compounds were per se not effective against Ba/F3 BCR-ABL[T315I] cells at clinically relevant concentrations (**Supplementary Results**, **Supplementary Table 1**). However, given that kinase inhibitors are generally known to share polypharmacologic features, we hypothesized that combining two agents that were initially not very efficacious could result in synergistic cell killing because of a cooperative effect of previously unappreciated off targets. Therefore, all possible pairwise combinations were tested in an effector concentration for a 20% maximal response (EC_{20}) by EC_{20} checkerboard design and evaluated by comparison of the experimentally derived impairment of cellular viability with the predicted combinatorial effect determined using the Bliss-additivity model (**Supplementary Table 2**)[19].

We observed a pronounced synergy between the pan–aurora kinase inhibitor danusertib and the dual ABL and SRC inhibitor bosutinib that we validated in detail by generating multifactorial dilutions of both agents, resulting in three-dimensional dose-response surfaces[20]. These were again correlated to the Bliss-predicted values. Calculating the differential volumes between the predicted and measured inhibitions allowed an estimation of synergy over a broad concentration range, where a positive interaction volume indicates synergy. We observed a strong synergism between danusertib and bosutinib in killing BCR-ABL[T315I]–transformed cells in the lower, clinically relevant dose range, reaching up to 40% more inhibition than predicted by Bliss additivity (**Fig. 1b**). To further investigate the specificity of the observed synergy, we tested the combination of danusertib and bosutinib in a BCR-ABL wild-type background as well as in parental Ba/F3 cells. Danusertib and bosutinib only synergized in the gatekeeper-mutant background. Furthermore, using a combination of dasatinib and tozasertib, compounds with overlapping cognate targets, the detected synergy could be mimicked only to a much lesser extent, suggesting the possibility that off-target effects were responsible for the observed synergy (**Fig. 1c**).

Synergy is conserved in primary cells harboring BCR-ABL[T315I]

We next asked whether the observed synergistic drug interaction is also conserved in a setting that is closer to the in vivo situation. Thus, we retrovirally transduced primary mouse bone-marrow cells with BCR-ABL[T315I], thereby rendering them growth-factor independent. A significant reduction ($P < 0.0001$) in colony-formation capability was observed in the presence of the drug combination as compared to the presence of either danusertib or bosutinib alone after 10 d of drug incubation (**Fig. 1d** and **Supplementary Fig. 1**). Moreover, the synergy between danusertib and bosutinib also translated into *ex vivo* proliferation assays using primary cells isolated from the peripheral blood of a patient suffering from advanced BCR-ABL[T315I]–positive CML (**Fig. 1e**). In line with the cell line–derived data, the cooperative drug interaction was not observed using primary cells from a BCR-ABL[WT]–positive patient (**Supplementary Fig. 2**). To rule out the possibility that the measured effect was caused solely by cooperative inhibitory effects on BCR-ABL[T315I] activity, *in vitro* kinase assays were performed. These studies showed a buffering effect of the drug combination that did not exceed the single-drug efficacy of danusertib, which was the more effective individual compound (**Supplementary Fig. 3**). By characterizing the impairment of cellular viability on Ba/F3 BCRABL[T315I] cells in more detail, we observed an increase in apoptosis that was specific in its collaborative nature for Ba/F3 BCR-ABL[T315I] cells. In fact, we observed a 13-fold increase in cleaved caspase 3 and caspase 7 in cells treated with the drug combination compared to vehicle-treated cells (**Fig. 1f** and **Supplementary Fig. 4**). Assessing the impact on the cell cycle after treatment with a single drug and with the drug combination, we detected a G2 arrest that was observed specifically for the drug combination in the mutant BCR-ABL background (**Supplementary Fig. 5**).

Multiple off targets implicated in Mapk signaling

With the intention of uncovering the off-target effects of the two agents that may underlie the observed synergy, a chemical proteomics approach was pursued as an initial step in deconvoluting potential targets. Chemical proteomics is a post-genomic version of drug affinity chromatography and is enabled by high-resolution tandem mass spectrometry and

downstream bioinformatics analysis[4]. Given that tozasertib and dasatinib, compounds that are related to danusertib and bosutinib, did not show a pronounced synergistic interaction, we hypothesized that the proteins underlying the cellular effect of the combination of danusertib and bosutinib would be specific binders of these drugs, thereby necessitating the identification of their cell-specific, proteome-wide target profiles. Analogs of all eight screened compounds were either available or designed for this study (**Supplementary Fig. 6**). For each compound, a modification that allowed immobilization on sepharose beads was introduced for the subsequent affinity purification of interacting proteins from lysates of the BCR-ABL^{T315I}–transformed Ba/F3 cells. Kinase-binding properties were not affected for any of the compounds, as confirmed by *in vitro* kinase assays for each analog compared to the parental small molecule (**Supplementary Table 3**). Using one-dimensional gel-free LC/MS chemical proteomics, a total of 68 protein kinase targets were identified for all 8 kinase inhibitors and, more specifically, 40 kinases bound to bosutinib and 37 kinases bound to danusertib in Ba/F3 BCR-ABL^{T315I} cell lysates (**Fig. 2a,b**). To quantify the relative affinities of the identified kinase binders to the eight small molecules, the chemical proteomics experiments were extended using the iTRAQ methodology (isobaric tag for relative and absolute quantitation)[21,22]. These experiments were subsequently analyzed by two-dimensional gel-free LC/MS.

Intensity ratios were obtained for 43 kinases (**Fig. 2c**, **Supplementary Fig. 7** and **Supplementary Data Set 2**). In addition to reproducing known target-ligand interactions, such as identifying Tec kinase as a specific interactor of dasatinib and confirming the higher affinity of both bosutinib and dasatinib for Src or Csk, we also identified kinase targets that would almost exclusively bind to only one of the agents tested. In particular, we found various kinases that are implicated in Mapk signaling, such as Mapk1 (Erk2), Map2k1 (Mek1), Map2k2 (Mek2), Map3k3 and Pyk2 (Ptk2b), that have a strong propensity for binding to either danusertib or bosutinib but not to the other inhibitors tested (**Fig. 2c** and **Supplementary Fig. 7**). To further support the chemical proteomics–derived data, we performed additional *in vitro* enzymatic assays and competitive binding experiments (**Supplementary Figs. 8** and **9**). A subsequent pathway analysis using all the identified targets of either danusertib or bosutinib alone as well as their collective target spectrum as queries suggested that both agents had a substantial impact on the Mapk signaling cascade, both individually and cooperatively[23]. Using the DAVID bioinformatics interface, we observed a significant enrichment for the drug combination in the KEGG (P = 8.98×10^{-9}, false discovery rate (FDR) = 9.2×10^{-6}) and BIOCARTA (P = 2.49×10^{-9}, FDR = 2.8×10^{-6}) Mapk pathways that was not achieved to the same extent by querying the single target spectra of either danusertib or bosutinib and therefore indicated that the impact of both drugs on this pathway was not of a redundant nature but, rather, was of a cooperative nature (**Supplementary Table 4**)[23].

c-Myc targets are downregulated on a genome-wide scale

Post-translational modification of transcription factors, which causes transcriptional activation through nuclear translocation, homodimerization or heterodimerization, is a common mechanism by which signaling cascades can integrate environmental stimuli into

altered transcriptional responses and, in turn, is an immediate answer by the cellular system to any given kind of intervention[24].

To determine the functional consequences of the simultaneous application of danusertib and bosutinib, we analyzed global transcriptional changes by generating differential gene expression profiles. Using the concentrations that resulted in the highest synergy, the impact of either of the drugs alone and their combination at an equal dose was compared to that of the vehicle control 6 h after drug exposure (**Supplementary Fig. 10**). At this time point, no signs of cell death or impaired cellular viability were detected (data not shown). Taking an FDR of 0.05 into consideration, there were no significantly regulated genes when Ba/F3 BCR-ABL^{T315I} cells were treated with 300 nM danusertib. Also, the number of significantly regulated genes resulting from treatment with 1 μM bosutinib was relatively low, with 26 upregulated and 12 downregulated genes. However, when both compounds were combined, severe alterations in the transcriptome were observed, with 645 genes significantly upregulated and 584 genes significantly downregulated (**Fig. 3a**, **Supplementary Fig. 11** and **Supplementary Data Set 1**). This observation supported the previous notion that the combined effect of both drugs is not explainable solely by the summation of the individual effects of the two agents alone and suggested that cooperative inactivation of a transcription factor might be linked to the observed cellular synergy. Therefore, we performed a database query with all significantly regulated genes in each measured condition using the Molecular Signature Database (MSigDB). Thus, the group of genes downregulated by the combined drug treatment was found to be specifically enriched for genes containing c-Myc regulatory motifs in their promoters (**Fig. 3b**).

To extend our findings, which were limited to the subset of significantly regulated genes, to the entire genome, we next conducted an unbiased gene set enrichment analysis[25] comparing all the conditions measured. This independent approach reproduced the finding that genes containing a c-Myc motif were strongly correlated with downregulation by combination drug treatment (**Fig. 3c**). Moreover, we evaluated the impact of the drug combination on an experimentally derived c-Myc transcriptional signature, which also revealed global downregulation of c-Myc–dependent target genes in the drug combination treatment as compared to DMSO treatment (**Fig. 3d**)[26].

Mapk signaling affected by drug action

We initially set out to investigate the consequence of single and combined drug treatment on the consensus BCR-ABL signaling network using immunoblotting (**Fig. 4a**). A gradual decrease in total phosphotyrosine levels, including BCR-ABL phosphorylation itself, was observed with both agents individually and in combination. Conversely, other well-known readouts for canonical BCRABL signaling, such as phosphorylation of Stat5 or Crkl, were not markedly impaired at the concentrations used and only decreased detectably when the concentrations of both compounds were increased fourfold (data not shown). As in a BCR-ABL wild-type signaling background, phosphorylated Stat5 (pStat5) and pCrkl are very sensitive readouts for BCR-ABL activity; this observation was unexpected and therefore necessitated a more unbiased, global phosphoproteomics approach (**Supplementary Fig. 12**). Using eight-plex iTRAQ, we assayed the four different treatment conditions (DMSO,

danusertib, bosutinib and the combination of danusertib and bosutinib) at an early, 15-min time point and a late, 6-h time point. Approximately 700 phosphopeptides could be quantified at both time points, including 110 phosphotyrosine peptides and 563 phosphoserine or phosphothreonine peptides. Because of the dynamic nature of phosphorylation, the early time point was more informative. Further analysis was therefore conducted using the 15-min treatment time as a reference. To identify common patterns of response of each site to treatment with a single drug or the drug combination, an unsupervised, self-organizing phylo-genetic clustering algorithm (SOTA) was applied that allocated each phosphopeptide to one unique cluster[27]. Thus, 11 distinct clusters of response patterns were identified that ranged from a completely unchanged phosphorylation status to cooperative downregulation of given phosphorylation sites and signaling cascades (**Fig. 4b**, **Supplementary Fig. 13** and **Supplementary Data Set 3**).

Subsequent pathway analysis of each separate cluster revealed enrichments for various pathways (**Supplementary Table 5**). Most notably, however, MAPK and CML pathways were specifically enriched ($P < 0.05$) in active response patterns, as represented in clusters 3, 4, 5 and 6. Notably, cluster 4 also contained phosphopep-tides for Mek (Ser222) and Erk (Tyr185) (**Fig. 4c** and **Supplementary Methods**). This is in line with the results from the proteome-wide target survey using chemical proteomics that suggested Mek and Erk as specific binders of bosutinib and danusertib, respectively. Phosphorylation of these sites correlates with the active states of the respective kinases. In addition to Mek and Erk, the quantitative phosphoproteomics analysis also revealed differentially altered phosphor-ylation events on other proteins implicated in the BCR-ABL–MAPK signaling network (**Supplementary Fig. 14**). To gain more confidence in the functional relevance of the inhibition of Map kinases in the context of the observed synergy, we assessed whether Ba/F3 BCR-ABL^{T315I} cells would be more sensitive toward their inhibition as compared to Ba/F3 BCR-ABL^{WT} cells. Using various small-molecule inhibitors, we observed a trend toward a higher sensitivity for Mapk pathway inhibition in BCR-ABL^{T315I} cells (**Supplementary Figs. 15** and **16**).

Moreover, factorial dilutions were prepared in which either danusertib or bosutinib was replaced with a tool compound for the respective targets of interest. Replacing bosutinib with U0126, a widely used Mek inhibitor, and replacing danusertib with Erk inhibitor II or the Pyk2 kinase inhibitor PF431396 preserved the initially obtained synergy in the higher dose ranges of the tool compounds. Pharmacological inhibition of Pyk2 resulted in reduced Erk phosphorylation (**Fig. 4d** and **Supplementary Figs. 17** and **18**).

Combined drug treatment impairs c-Myc activity

Following up on the transcriptome analysis, we investigated the molecular logic of the global downregulation of c-Myc target genes and the possible consequences of this downregulation on cellular fitness. *c-Myc* itself was among the most significantly downregulated genes, which was validated by quantitative RT-PCR. (**Fig. 5a** and **Supplementary Fig. 19**). Notably, this did not translate to downregulation of c-Myc protein until 48 h of drug treatment (**Supplementary Fig. 20a**). Thus, the downregulation at the mRNA level and the functional consequence of overall downregulation of c-Myc–dependent

transcriptional networks seem to be independent events. To examine the possibility that the reduction in target gene expression was a result of altered cellular localization of c-Myc, nuclear extracts were generated after 48 h of combined drug treatment and were compared with vehicle-treated controls (**Supplementary Fig. 20b**). No obvious differences in nuclear localization were apparent, which is indicative of another mechanism of action. Intersecting the quantitative phosphoproteomics profiles with the transcriptomics data highlighted the Mapk signaling cascade, which was one of the most substantially affected pathways, as one of the most prominent upstream pathways of c-Myc. Erk is known to phosphorylate c-Myc at Ser62, which correlates with the transcriptional activity of c-Myc[28–31]. Hence, an immuno-blot ana lysis of pErk (phosphorylated at Thr202 and Tyr204) was performed to validate the impact of the combined drug treatment on Mapk signaling (**Fig. 5b**). Both compounds showed relatively similar effects on their own and cooperativity when combined, thus validating the findings of the large-scale phosphoproteomics data set. In comparison, the dynamics of the phosphorylation of Ser62 were affected in a way that only the combined application of both kinase inhibitors had a measurable effect (**Fig. 5b** and **Supplementary Fig. 21**). To test whether this observation also translates into functional impairment of c-Myc activity, ELISA-based binding assays were performed using nuclear extracts from Ba/F3 BCR-ABL^{T315I} cells that were treated for 2 h with vehicle, single compounds or their combination to assess Myc binding to spotted double-stranded oligos that contain c-Myc consensus binding sites. Whereas danusertib and bosutinib alone had only a relatively mild impact on the binding of endogenous c-Myc to its consensus sequence, the combination treatment significantly ($P < 0.005$) reduced binding affinity at equal c-Myc loading (**Fig. 5c** and **Supplementary Fig. 22**). To further study the impact of targeting c-Myc in BCR-ABL^{T315I}–dependent cells, we used JQ1, a recently described BRD4 inhibitor that downregulates c-Myc on both the mRNA and protein levels[32,33]. Notably, only the active enantiomer JQ1S reduced c-Myc mRNA levels in Ba/F3 BCR-ABL^{T315I} cells, whereas treatment with the inactive enantiomer JQ1R did not (**Supplementary Fig. 23**). Consistently, only JQ1S reduced cellular viability, thus independently validating the dependence of Ba/F3 BCR-ABL^{T315I} cells on c-Myc (**Fig. 5d**).

DISCUSSION

We describe a systems-wide approach aimed at capturing and exploring the molecular mechanisms behind the synergistic drug-drug interaction of the clinical kinase inhibitors danusertib and bosutinib. This synergy was specific for CML cells featuring the BCR-ABL^{T315I} gatekeeper mutation and thus addresses an unmet medical need, as this mutation confers resistance to all currently approved kinase inhibitors for CML. The approach of integrating mass spectrometry–based target profiles with phosphoproteomic and transcriptional data sets should have broad applicability to other disease settings and biological questions.

The specificity of the observed synergistic drug interaction for the BCR-ABL^{T315I} gatekeeper-transformed cells over BCR-ABL wild-type cells was perhaps surprising. At least two explanations for this relationship seem feasible. One possible explanation might be that each drug is already highly potent against BCR-ABL wild-type– transformed cells, which may mask any other effect and make the detection of cooperative effects on

downstream pathways technically difficult. Another explanation may be qualitative changes in the signaling properties of BCR-ABL^{T315I} as compared to wild-type BCR-ABL. Monitoring the cellular markers of wild-type BCR-ABL activity through careful titration of drug inhibition or stepwise induction of BCR-ABL expression has shown that phosphorylation of Stat5 is the most sensitive cellular readout for BCR-ABL kinase activity, followed by total phosphotyrosine levels and, finally, phosphorylation of Crkl (ref. 34). In BCR-ABL^{T315I} mutant cells, however, we found pStat5 and pCrkl levels to be relatively insensitive to BCRABL^{T315I} inhibition. Instead, BCR-ABL^{T315I} seemed to depend more strongly on Mapk signaling, as combined targeting of this pathway by bosutinib and danusertib conferred increased sensitivity. This seems consistent with qualitative changes in the signaling properties of BCR-ABL with mutations in the gatekeeper residue in addition to quantitative effects that may be cell-type and assay dependent[35,36]. Though we found a heightened dependence on, but not enhanced activity of, Map kinases in BCR-ABL^{T315I} cells, these may be related phenomena, and they highlight the particular synergy between the BCR-ABL and the Mapk pathways[18].

Both chemical proteomics and phosphoproteomics analyses suggested bosutinib as an inhibitor of the BCR-ABL gatekeeper kinase activity, which was subsequently confirmed by immuno-blotting and *in vitro* kinase assays. It is, however, important to note that this enzymatic inhibition did not translate into substantial cellular efficacy of bosutinib in the context of BCR-ABL^{T315I}–positive CML, which is consistent with clinical reports[37]. This might indicate activation of an unknown downstream roadblock by bosutinib through one of its multiple off targets. It is also noteworthy that, although danusertib and bosutinib both inhibit BCR-ABL^{T315I} kinase activity, combination *in vitro* kinase assays suggested that the observed synergy was not based on cooperativity in regard to the inhibition of BCR-ABL^{T315I} itself. Therefore, this effect must be predominantly attributed to inhibition of other targets.

Our observations converge on the Mapk signaling cascade as the predominantly affected pathway of the synergistic drug combination. Chemical proteomics identified several Map3ks, Map4ks and, particularly, Mek1 and Mek2 as specific targets of bosutinib, whereas Erk1 and Erk2 interacted exclusively with danusertib. In addition, Pyk2 (Ptk2b), one of the most prominent targets of danusertib (half-maximal inhibitory concentration (IC$_{50}$) = 79.9 nM; **Supplementary Fig. 8**), is known to also feed into Mapk signaling through Erk phosphorylation (**Supplementary Fig. 18**). Although BCR-ABL^{T315I} was bound by both drugs, the global phosphoproteome survey showed little combinatorial drug effects on canonical BCR-ABL downstream signals other than those culminating in the Mapk pathway, especially Gab2 Ser604, Mek1 Ser222 and Erk2 Tyr185. Querying the drug-dependent transcriptomic signature for significantly (P < 0.01) regulated transcription factor motifs highlighted c-Myc as a crucial factor in transmitting the cellular response to combined treatment with danusertib and bosutinib.

Myc has a well-established, but still not completely understood, role in a broad spectrum of human cancers because of its highly promiscuous features[38]. In the context of CML, c-Myc is required for BCR-ABL–mediated transformation[39]. It has also been reported as an essential gene in CML cell lines and has been linked to the clinical response to imatinib[40,41].

Because of the lack of a chemically tractable enzymatic function, pharmacological targeting of c-Myc is a formidable challenge for which promising steps have only recently been made[32,33]. The BRD4-targeting compound JQ1 seems to suppress mainly transcriptional expression of c-Myc. We have not been able to obtain reliable results in our attempts to downregulate c-Myc by alternative methods, such as inducible RNA expression, probably because c-Myc is essential for cellular survival. We found that combined drug treatment with bosutinib and danusertib led to reduced engagement of c-Myc DNA binding sites and downregulation of c-Myc target genes. Our results indicate regulation of c-Myc activity at the post-translational level. C-Myc is known to be phosphorylated on several N-terminal residues that are linked to protein stability and transcriptional activity[42]. Ser62 phosphorylation, which is known to be mediated by MAP kinase signaling[43], is among the most prominent post-translational modifications, and although it has been mainly described as a stabilizing event, there is evidence that it has a direct role in modulating transcriptional activity[30,43].

The ability to effectively integrate large omics data sets to elucidate the molecular effects of genetic or chemical perturbation of biological systems remains a challenge. This is particularly true for the application of multiple pharmacological agents[44]. The approach described here is empowered by the use of quantitative mass spectrometry–derived chemical proteomics profiling of the cellular targets of compounds. The obtained 'physical' link between the perturbing agent and the cellular repertoire of molecules is sufficiently direct and reliable to represent a strong vantage point for subsequent integration with other data sets through the use of network and pathway analysis. We have thus been able to elucidate the impact of a new synergistic drug interaction in a clinically relevant, highly drug-resistant disease setting. The study revealed a nonobvious synergistic mechanism of action that is elicited by several off targets of the two small molecules. Thus, the polypharmacology of kinase inhibitors with good safety profiles represents, in this case, an advantage that allows for their versatile and combinatorial use in the quest for stratified cancer therapy[6,7].

METHODS

Cell lines and reagents

The parental Ba/F3 cell line was obtained from the American Type Culture Collection and was cultured in RPMI and 10% fetal calf serum (FCS). Imatinib, nilotinib, dasatinib, bosutinib and tozasertib were purchased from LC Laboratories. Danusertib, CI-1040, AZD6244 and sorafenib were purchased from Selleck Chemicals. Bafetinib, c-bafetinib, c-dasatinib, c-nilotinib and c-tozasertib were synthesized by WuXi AppTec. C-imatinib, c-sorafenib, c-bosutinib and c-danusertib were synthesized by Siokem, Gateway Pharma, Vichem Chemie and AMRI, respectively. C-imatinib, c-nilotinib, c-bafetinib and c-sorafenib were esterified with N-Boc-glycine and deprotected with trifluoroacetic acid as part of the coupling procedure. U0126 and Erk inhibitor II were purchased from Sigma-Aldrich and Calbiochem, respectively. PF431396 was purchased from Tocris. JQ1S and JQ1R were kindly provided by J. Bradner (Dana-Farber Cancer Institute, Boston, Massachusetts, USA). The purity (>94%) of all compounds was confirmed using HPLC and MS analysis. All compounds were dissolved in DMSO as 10 mM stock solutions. Further chemical

characterization data for c-imatinib, c-nilotinib, c-bafetinib, c-sorafenib and c-danusertib can be found in the **Supplementary Methods**.

Immunoblot analysis

Immunoblotting was performed according to the manufacturer's recommendations for antibodies to pStat5A and pStatB (1:1,000, Tyr694 and Tyr699 for pStat5A and pStat5B, respectively; 94-10C-9-10C-2, Millipore); pSrc family (1:1,000, Tyr416, 2101, Cell Signaling Technology); pCrkl (1:1,000, Tyr207, 3181, Cell Signaling Technology); actin (1:2,000, AAN01, Cytoskeleton); Abl (1:1,000, Ab-3, Calbiochem); total phosphotyrosine 4G10 (1:2,000, Upstate Biotechnology); total Myc (1:7,000, IR-Dye800 conjugated a-Myc epitope tag (Rb), 600-432-381, Rockland); pMyc (1:1,000, Ser62, ab51156, Abcam); Erk1 and Erk2 (1:2,500, M5670, Sigma-Aldrich); pErk1 and pErk2 (1:1,000, Thr202 and Tyr204 for isoforms 1 and 2, respectively, 9106, Cell Signaling Technology); and Rcc-1 (1:1,000, sc-55559, Santa Cruz).

Viability assays and synergy determination

Viability assays were performed in triplicates using the Cell Titer Glo assay (Promega) after 72 h of drug exposure to cells initially seeded at a density of 10^5 cells per ml. Point-wise synergy screening was performed by deriving EC_{20} values for each compound and combining them in every possible pairwise combination. Experimentally derived values were compared with values predicted by the Bliss additivity model[19]. Thirty-six–point dose-response matrices have been established and evaluated as described elsewhere[20].

Proteomics analysis and MS strategies

More detailed information on the immobilization of small molecules, affinity purification, tryptic digestion, peptide purification, iTRAQ labeling and liquid chromatography, as well as data extraction, database searching and relative quantification, is outlined in the **Supplementary Methods**.

Apoptosis and cell-cycle measurements

Induction of apoptosis was measured 16 h after drug exposure using the Caspase Glo assay (Promega) measuring the cleavage of caspase 3 and caspase 7. Experiments were performed in triplicate. The cell-cycle analysis was performed by staining DNA with propidium iodide after 36 h of exposure to the respective drugs.

Colony formation assay

After retroviral transduction of primary mouse bone marrow cells with BCR-ABL^{T315I} internal ribosomal entry site GFP, GFP-positive cells were isolated using fluorescence-activated cell sorting and seeded in cytokine-free methylcellulose. Colonies were scored after 10 d.

Ex vivo proliferation assays using primary patient material

Primary cells were obtained from the bone marrow of two patients with advanced BCR-ABL^{T315I} CML and one patient with advanced CML and no detectable BCR-ABL mutation.

Mononuclear cells were isolated using Ficoll. They were then incubated in triplicate in RPMI 1640 medium with FCS in the presence or absence of various concentrations of bosutinib or danusertib, either as single agents or in combination at a fixed ratio of drug concentrations at 37 °C for 48 h. After incubation, ^{3}H-thymidine (PerkinElmer; 0.5 [.Mu]Ci per well) was added for another 16 h. Cells were then harvested on filter membranes (Packard Bioscience) in a Filtermate 196 harvester (Packard Bioscience). Filters were then air dried, and the bound radioactivity was measured in a β-counter (Top-Count NXT, Packard Bioscience).

Kinase assays

Kinase assays for BCR-ABL^{T315I}, AURKA (c-danusertib) and PDGFRA (c-sorafenib) were performed using the KinaseProfiler (Millipore). PYK2 inhibition by danusertib was assessed using the SelectScreen ZLYTE platform (Life Technologies). MAP2K5 and MAP3K3 kinase assays were conducted with the STK-ELISA platform (Carna Biosciences). CDK7 and NEK9 kinase assays were conducted using the off-chip Mobility Shift Assay (Carna Biosciences). C-imatinib and c-nilotinib were assayed *in vitro* for inhibition of recombinant full-length c-ABL (Upstate Biotechnology), as described previously[45]. All kinase assays were performed using ATP concentrations that approximately equaled the K_m of the respective kinase.

Microarray analysis

Information on treatment conditions and data handling can be found in the **Supplementary Methods**.

MYC binding assays

Binding of endogenous c-MYC to its consensus sites was assessed by TransAM DNA binding ELISA assays (Active Motif, 43396) according to the manufacturer's recommendations.

Statistics

Two-tailed t tests were used for statistical analyses, and a difference was considered significant when $P < 0.05$. Further statistical considerations of the data-analysis tools used in the manuscript are provided either in the

Supplementary Material

Refer to Web version on PubMed Central for supplementary material.

Acknowledgments

References

1. Kitano H. Cancer as a robust system: implications for anticancer therapy. Nat. Rev. Cancer. 2004; 4:227–235. [PubMed: 14993904]

2. Lehár J, et al. Synergistic drug combinations tend to improve therapeutically relevant selectivity. Nat. Biotechnol. 2009; 27:659–666. [PubMed: 19581876]

3. Lamb J, et al. The Connectivity Map: using gene-expression signatures to connect small molecules, genes, and disease. Science. 2006; 313:1929–1935. [PubMed: 17008526]

4. Rix U, Superti-Furga G. Target profiling of small molecules by chemical proteomics. Nat. Chem. Biol. 2009; 5:616–624. [PubMed: 19690537]

5. Pan C, Olsen JV, Daub H, Mann M. Global effects of (inase inhibitors on signaling networks revealed by quantitative phosphoproteomics. Mol. Cell. Proteomics. 2009; 8:2796–2808. [PubMed: 19651622]

6. Hopkins AL. Network pharmacology: the next paradigm in drug discovery. Nat. Chem. Biol. 2008; 4:682–690. [PubMed: 18936753]

7. Knight ZA, Lin H, Shokat KM. Targeting the cancer kinome through polypharmacology. Nat. Rev. Cancer. 2010; 10:130–137. [PubMed: 20094047]

8. Quintás-Cardama A, Cortes J. Molecular biology of BCR-ABL1–positive chronic myeloid leukemia. Blood. 2009; 113:1619–1630. [PubMed: 18827185]

9. Druker BJ. Imatinib as a paradigm of targeted therapies. Adv. Cancer Res. 2004; 91:1–30. [PubMed: 15327887]

10. Gorre ME, et al. Clinical resistance to STI-571 cancer therapy caused by BCR-ABL gene mutation or amplification. Science. 2001; 293:876–880. [PubMed: 11423618]

11. Donato NJ, et al. Imatinib mesylate resistance through BCR-ABL independence in chronic myelogenous leukemia. Cancer Res. 2004; 64:672–677. erratum 64, 2306 (2004). [PubMed: 14744784]

12. Mahon FX, et al. Selection and characterization of BCR-ABL positive cell lines with differential sensitivity to the tyrosine kinase inhibitor STI571: diverse mechanisms of resistance. Blood. 2000; 96:1070–1079. [PubMed: 10910924]

13. Zhang J, Yang PL, Gray NS. Targeting cancer with small molecule kinase inhibitors. Nat. Rev. Cancer. 2009; 9:28–39. [PubMed: 19104514]

14. Bixby D, Talpaz M. Seeking the causes and solutions to imatinib-resistance in chronic myeloid leukemia. Leukemia. 2011; 25:7–22. [PubMed: 21102425]

15. O'Hare T, et al. AP24534, a pan–BCR-ABL inhibitor for chronic myeloid leukemia, potently inhibits the T315I mutant and overcomes mutation-based resistance. Cancer Cell. 2009; 16:401–412. [PubMed: 19878872]

16. Eide CA, et al. The ABL switch control inhibitor DCC-2036 is active against the chronic myeloid leukemia mutant BCR-ABLT315I and exhibits a narrow resistance profile. Cancer Res. 2011; 71:3189–3195. [PubMed: 21505103]

17. Grebien F, et al. Targeting the SH2-kinase interface in Bcr-Abl inhibits leukemogenesis. Cell. 2011; 147:306–319. [PubMed: 22000011]

18. Packer LM, et al. Nilotinib and MEK inhibitors induce synthetic lethality through paradoxical activation of RAF in drug-resistant chronic myeloid leukemia. Cancer Cell. 2011; 20:715–727. [PubMed: 22169110]

19. Bliss CI. The toxicity of poisons applied jointly. Ann. Appl. Biol. 1939; 26:585–615.

20. Borisy AA, et al. Systematic discovery of multicomponent therapeutics. Proc. Natl. Acad. Sci. USA. 2003; 100:7977–7982. [PubMed: 12799470]

21. Breitwieser FP, et al. General statistical modeling of data from protein relative expression isobaric tags. J. Proteome Res. 2011; 10:2758–2766. [PubMed: 21526793]

22. Ross PL, et al. Multiplexed protein quantitation in Saccharomyces cerevisiae using amine-reactive isobaric tagging reagents. Mol. Cell. Proteomics. 2004; 3:1154–1169. [PubMed: 15385600]

23. Dennis G Jr. et al. DAVID: Database for Annotation, Visualization, and Integrated Discovery. Genome Biol. 2003; 4:P3. [PubMed: 12734009]

24. Chen X, et al. Integration of external signaling pathways with the core transcriptional network in embryonic stem cells. Cell. 2008; 133:1106–1117. [PubMed: 18555785]

25. Subramanian A, et al. Gene set enrichment analysis: a knowledge-based approach for interpreting genome-wide expression profiles. Proc. Natl. Acad. Sci. USA. 2005; 102:15545–15550. [PubMed: 16199517]

26. Schuhmacher M, et al. The transcriptional program of a human B cell line in response to Myc. Nucleic Acids Res. 2001; 29:397–406. [PubMed: 11139609]

27. Dopazo J, Carazo JM. Phylogenetic reconstruction using an unsupervised growing neural network that adopts the topology of a phylogenetic tree. J. Mol. Evol. 1997; 44:226–233. [PubMed: 9069183]

28. Gupta S, Seth A, Davis RJ. Transactivation of gene expression by Myc is inhibited by mutation at the phosphorylation sites Thr-58 and Ser-62. Proc. Natl. Acad. Sci. USA. 1993; 90:3216–3220. [PubMed: 8386367]

29. Seth A, Alvarez E, Gupta S, Davis RJ. A phosphorylation site located in the NH_2-terminal domain of c-Myc increases transactivation of gene expression. J. Biol. Chem. 1991; 266:23521–23524. [PubMed: 1748630]

30. Hann SR. Role of post-translational modifications in regulating c-Myc proteolysis, transcriptional activity and biological function. Semin. Cancer Biol. 2006; 16:288–302. [PubMed: 16938463]

31. Benassi B, et al. c-Myc phosphorylation is required for cellular response to oxidative stress. Mol. Cell. 2006; 21:509–519. [PubMed: 16483932]

32. Delmore JE, et al. BET bromodomain inhibition as a therapeutic strategy to target c-Myc. Cell. 2011; 146:904–917. [PubMed: 21889194]

33. Filippakopoulos P, et al. Selective inhibition of BET bromodomains. Nature. 2010; 468:1067–1073. [PubMed: 20871596]

34. Hantschel O, et al. BCR-ABL uncouples canonical JAK2-STAT5 signaling in chronic myeloid leukemia. Nat. Chem. Biol. 2012; 8:285–293. [PubMed: 22286129]

35. Griswold IJ, et al. Kinase domain mutants of Bcr-Abl exhibit altered transformation potency, kinase activity, and substrate utilization, irrespective of sensitivity to imatinib. Mol. Cell. Biol. 2006; 26:6082–6093. [PubMed: 16880519]

36. Azam M, Seeliger MA, Gray NS, Kuriyan J, Daley GQ. Activation of tyrosine kinases by mutation of the gatekeeper threonine. Nat. Struct. Mol. Biol. 2008; 15:1109–1118. [PubMed: 18794843]

37. Cortes JE, et al. Safety and efficacy of bosutinib (SKI-606) in chronic phase Philadelphia chromosome-positive chronic myeloid leukemia patients with resistance or intolerance to imatinib. Blood. 2011; 118:4567–4576. [PubMed: 21865346]

38. Pelengaris S, Khan M, Evan G. c-MYC: more than just a matter of life and death. Nat. Rev. Cancer. 2002; 2:764–776. [PubMed: 12360279]

39. Sawyers CL, Callahan W, Witte ON. Dominant negative MYC blocks transformation by ABL oncogenes. Cell. 1992; 70:901–910. [PubMed: 1525828]

40. Luo B, et al. Highly parallel identification of essential genes in cancer cells. Proc. Natl. Acad. Sci. USA. 2008; 105:20380–20385. [PubMed: 19091943]

41. Albajar M, et al. MYC in chronic myeloid leukemia: induction of aberrant DNA synthesis and association with poor response to imatinib. Mol. Cancer Res. 2011; 9:564–576. [PubMed: 21460180]

42. Adhikary S, Eilers M. Transcriptional regulation and transformation by Myc proteins. Nat. Rev. Mol. Cell Biol. 2005; 6:635–645. [PubMed: 16064138]

43. Meyer N, Penn LZ. Reflecting on 25 years with MYC. Nat. Rev. Cancer. 2008; 8:976–990. [PubMed: 19029958]

44. Palsson B, Zengler K. The challenges of integrating multi-omic data sets. Nat. Chem. Biol. 2010; 6:787–789. [PubMed: 20976870]

45. Rix U, et al. A comprehensive target selectivity survey of the BCR-ABL kinase inhibitor INNO-406 by kinase profiling and chemical proteomics in chronic myeloid leukemia cells. Leukemia. 2010; 24:44–50. [PubMed: 19890374]
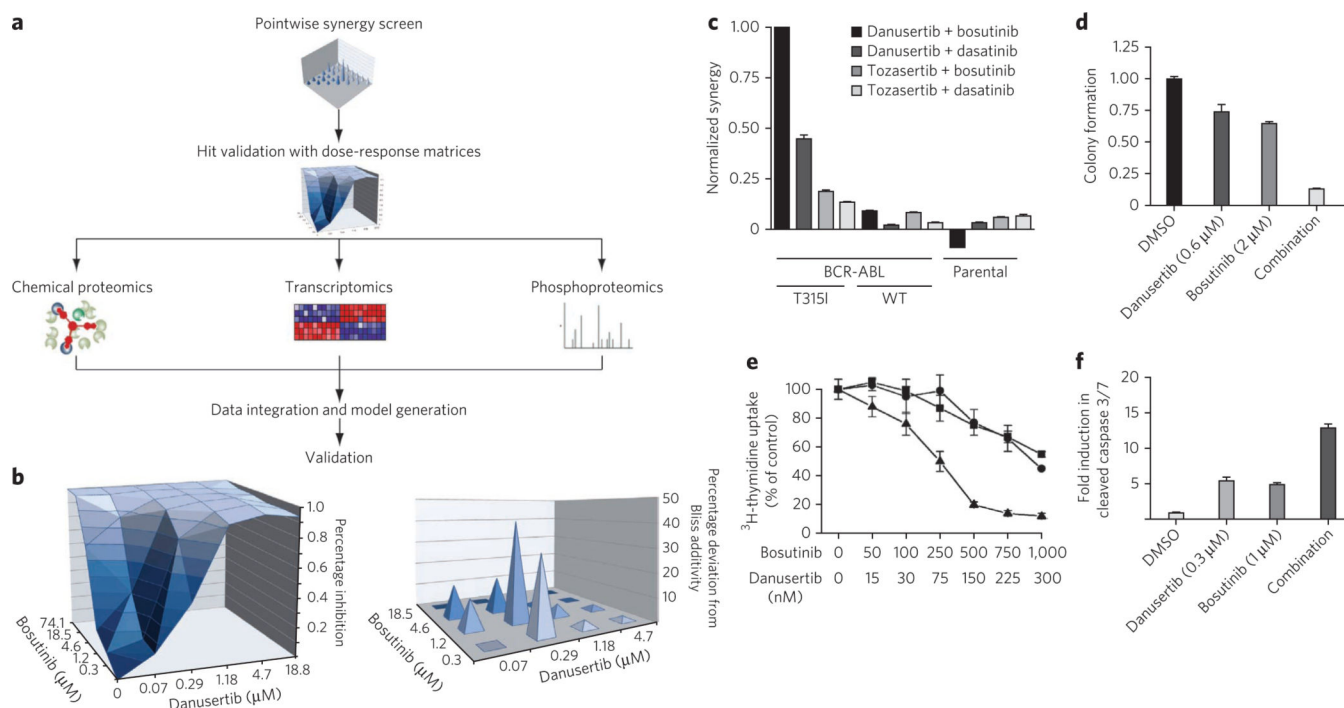
Figure 1. Danusertib and bosutinib synergize specifically in BCR-ABL^{T315I} cells
(**a**) Schematic outline of the three-pronged approach for comprehensive capturing of the cellular response to the combined drug treatment. (**b**) The combined effect of danusertib and bosutinib in Ba/F3 BCR-ABL^{T315I} cells exceeds the Bliss prediction, indicating a synergistic interaction. Needle graphs depict deviation from the Bliss-predicted additivity and represent the mean of triplicates. (**c**) Comparison of the differential volumes between experimentally derived and Bliss-predicted values. Data are the mean ± s.d. of triplicates. WT, wild type. (**d**) Colony formation capability of primary cells retrovirally transduced with BCR-ABL^{T315I} after drug treatment. Data represent the mean ± s.d. of quadruplicates. (**e**) ^{3}H-thymidine uptake in primary cells from the peripheral blood of a patient with BCR-ABL^{T315I}–positive CML that were incubated with bosutinib (■-■) and danusertib (#24Cf-#24Cf) as single agents or in combination (at a 10:3 fixed ratio of drug concentrations; ▲-▲). (**f**) Induction of apoptosis as measured by cleavage of caspase 3 and caspase 7 (caspase 3/7). Data depict fold increases and are the mean ± s.d. of triplicates.
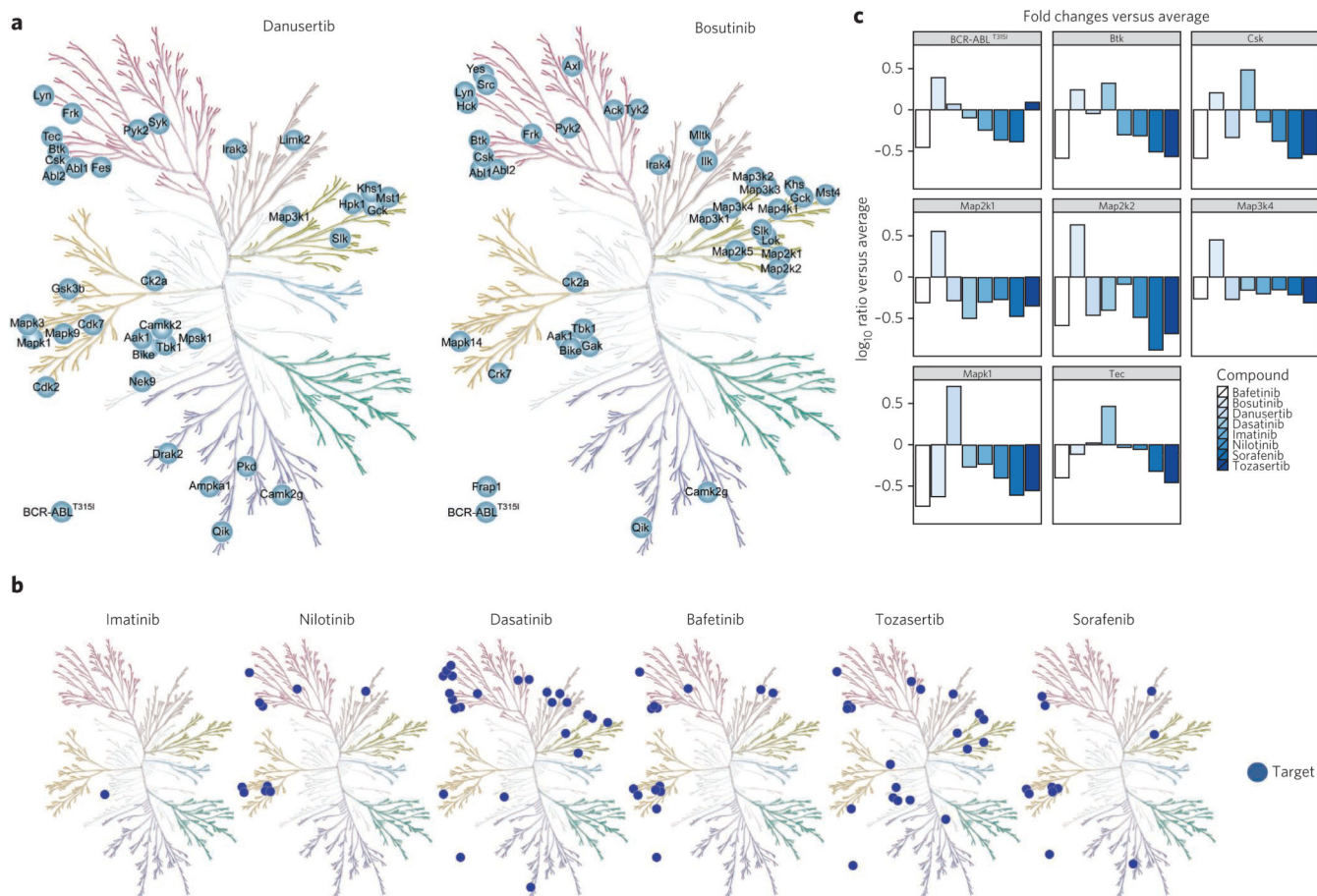
Figure 2. Quantitative chemical proteomics reveals target spectra of eight clinical BCR-ABL kinase inhibitors and indicates impairment of MAPK signaling resulting from off-target effects of danusertib and bosutinib

(**a**) Comprehensive kinase target profiles of danusertib and bosutinib as determined by gel-free one-dimensional LC/MS analysis mapped onto the human protein kinome. The human kinome is reproduced courtesy of Cell Signaling Technology (http://www.cellsignal.com/). (**b**) Kinome-wide target spectra of the remaining six kinase inhibitors used in this study as determined by one-dimensional LC/MS. (**c**) Bar graph depiction of eight-plex iTRAQ ratios for selected kinases (for the full panel of identified kinases, see **Supplementary Fig. 7**). Intensities were quantified using the average reporter tag intensity as a reference.
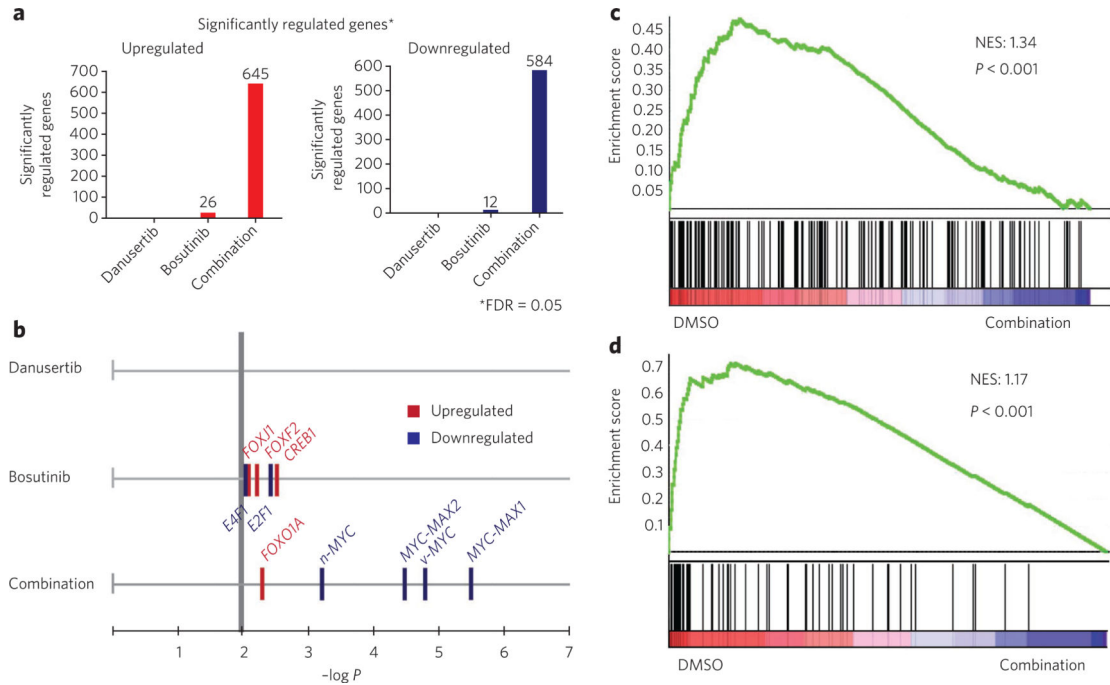
Figure 3. Transcriptome-wide analysis indicates global downregulation of *c-Myc* target genes after combinatorial treatment with danusertib and bosutinib

(**a**) Bar graphs showing the number of significantly upregulated and downregulated genes in each comparative condition. (**b**) *P* values for the enrichment of motif gene sets (MSigDB) only taking significantly (FDR < 0.05) regulated genes into consideration. (**c,d**) Gene set enrichment analysis showing global downregulation of genes with *c-MYC* regulatory motifs (**c**) and experimentally validated *c-Myc* target genes (**d**). NES, normalized enrichment score.
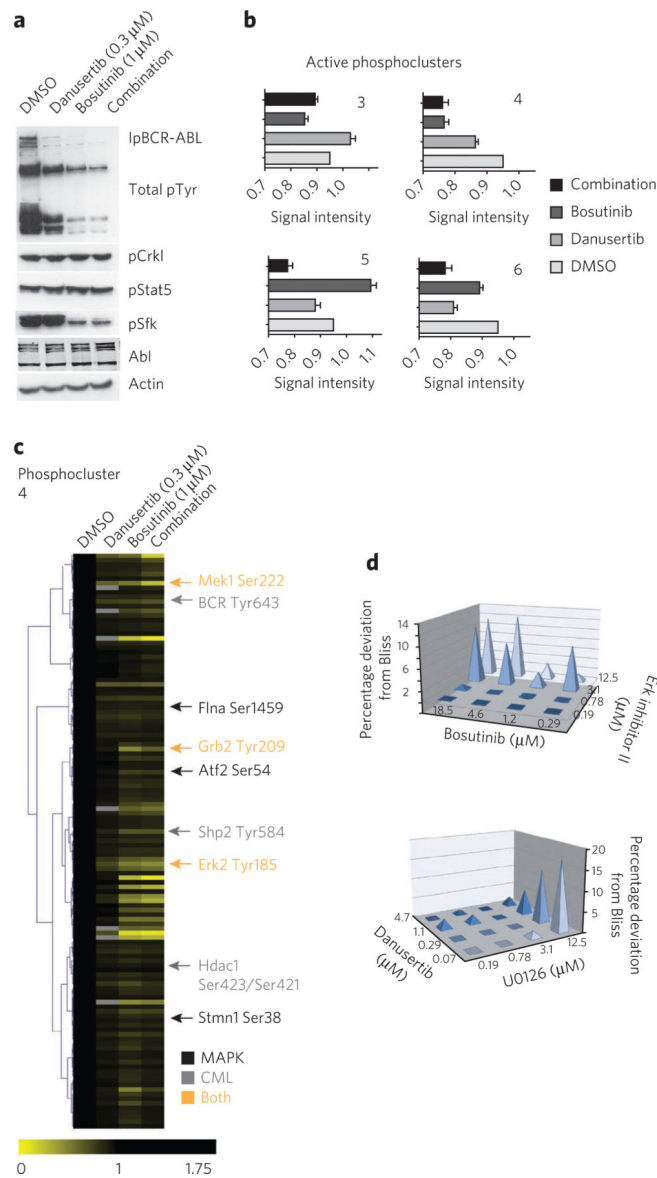
Figure 4. Quantitative phosphoproteomics highlights the impact of drug combination on the MAPK signaling network and the functional relevance of inhibition of MEK and ERK
(**a**) Immunoblot of total phosphotyrosine (pTyr), pCrkl, pStat5, pSfk (Src family kinases), Abl and actin of Ba/F3 BCR-ABL^{T315I} cells treated as indicated for 2 h. (**b**) SOTA analysis yielding 11 clusters of differential drug response patterns for the observed phosphopeptides, four of which (clusters 3, 4, 5 and 6) are considered to be active clusters. All clusters are represented in **Supplementary Figure 13**. (**c**) Heatmap rendition of all phosphorylation sites comprising active SOTA cluster 4, which is enriched for members of the MAPK (black) and CML (gray) signaling pathways. Phosphopeptide signatures corresponding to proteins that participate in both pathways are highlighted in orange. (**d**) Synergy of danusertib and bosutinib can be mimicked by the replacement of danusertib with ERK inhibitor II and of bosutinib with the MEK inhibitor U0126, respectively. Needle graphs

depict deviation from the Bliss-predicted additivity and represent the mean of triplicates. Raw immunoblot data for **a** are shown in **Supplementary Figure 24**.
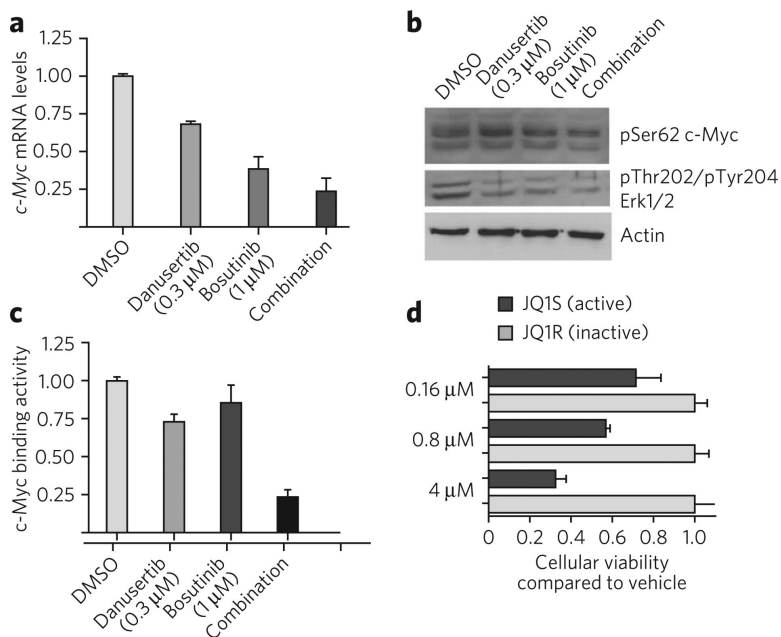
Figure 5. Combination of danusertib and bosutinib interferes on a post-translational level with *c-Myc* transcriptional activity.

(**a**) *c-Myc* mRNA levels after combined drug treatment for 6 h. Results represent the mean ± s.d. of triplicates. (**b**) Immunoblot of c-Myc phosphorylated at Ser62 (c-Myc pSer62), Erk1 and Erk2 phosphorylated at Thr202 and Tyr204, respectively (pThr202/pTyr204) and actin of Ba/F3 BCR-ABL^{T315I} cells treated as indicated for 2 h. (**c**) DNA binding activity of endogenous c-Myc determined by ELISA. Data are the mean ± s.d. of triplicates. (**d**) Viability of Ba/F3 BCR-ABL^{T315I} cells treated as indicated for 72 h. Results represent the mean ± s.d. of triplicates. Raw immunoblot data for **b** are shown in **Supplementary Figure 24**.